Available online at www.sciencedirect.com
ScienceDirect
Geochimica et Cosmochimica Acta 71 (2007) 129–144
Geochimica
www.elsevier.com/locate/gca

Enriched stable carbon isotopes in the pore waters of carbonate sediments dominated by seagrasses: Evidence for coupled carbonate dissolution and reprecipitation

Xinping Hu, David J. Burdige *

Department of Ocean, Earth and Atmospheric Sciences, Old Dominion University, Norfolk, VA 23529, USA

Received 16 March 2006; accepted in revised form 31 August 2006

Abstract

Studies of the $\delta^{13}C$ of pore water dissolved inorganic carbon ($\delta^{13}C$-DIC) were carried out in shallow water carbonate sediments of the Great Bahamas Bank (GBB) to further examine sediment–seagrass relationships and to more quantitatively describe the couplings between organic matter remineralization and sediment carbonate diagenesis. At all sites studied $\delta^{13}C$-DIC provided evidence for the dissolution of sediment carbonate mediated by metabolic CO_2 (i.e., CO_2 produced during sediment organic matter remineralization); these observations are also consistent with pore water profiles of alkalinity, total DIC and Ca^{2+} at these sites. In bare oolitic sands, isotope mass balance further indicates that the sediment organic matter undergoing remineralization is a mixture of water column detritus and seagrass material; in sediments with intermediate seagrass densities, seagrass derived material appears to be the predominant source of organic matter undergoing remineralization. However, in sediments with high seagrass densities, the pore water $\delta^{13}C$-DIC data cannot be simply explained by dissolution of sediment carbonate mediated by metabolic CO_2, regardless of the organic matter type. Rather, these results suggest that dissolution of metastable carbonate phases occurs in conjunction with reprecipitation of more stable carbonate phases. Simple closed system calculations support this suggestion, and are broadly consistent with results from more eutrophic Florida Bay sediments, where evidence of this type of carbonate dissolution/reprecipitation has also been observed. In conjunction with our previous work in the Bahamas, these observations provide further evidence for the important role that seagrasses play in mediating early diagenetic processes in tropical shallow water carbonate sediments. At the same time, when these results are compared with results from other terrigenous coastal sediments, as well as supralysoclinal carbonate-rich deep-sea sediments, they suggest that carbonate dissolution/reprecipitation may be more important than previously thought, in general, in the early diagenesis of marine sediments.

1. Introduction

Remineralization of sedimentary organic matter by aerobic respiration produces metabolic CO_2, and in undersaturated pore waters this CO_2 can react with carbonate sediments and cause their dissolution (see, e.g., Burdige and Zimmerman, 2002; Emerson and Bender, 1981, for further details). Approximating sediment organic matter as "CH_2O", these processes can be expressed as,

$$CH_2O + O_2 \rightarrow CO_2 + H_2O \quad (1)$$

$$CO_2 + CaCO_3 + H_2O \rightarrow Ca^{2+} + 2HCO_3^- \quad (2)$$

$$CH_2O + O_2 + CaCO_3 \rightarrow Ca^{2+} + 2HCO_3^- \quad (3)$$

and the coupling of aerobic respiration and carbonate dissolution implies that both processes can contribute to the pore water DIC pool. Our past studies (Burdige and Zimmerman, 2002) have also shown that seagrasses may enhance the dissolution of carbonate sediments when photosynthetically produced O_2 is "pumped" into the sediments through root and rhizome tissues and therefore promotes aerobic respiration in the sediments (i.e., rxn. 1).

* Corresponding author. Fax: +1 757 683 5303.
E-mail address: dburdige@odu.edu (D.J. Burdige).

0016-7037/$ - see front matter © 2006 Elsevier Inc. All rights reserved.
doi:10.1016/j.gca.2006.08.043

This O_2 input by seagrasses may also help to resolve the mass balance problem observed in some carbonate sediments between the extent of sediment carbonate dissolution and the amount of oxidant needed to produce the necessary amount of acid (Ku et al., 1999; Walter and Burton, 1990).

Because of the difference in stable carbon isotope signatures ($\delta^{13}C$) of marine organic carbon (approximately −17‰ to −23‰ PDB) and calcium carbonate (~0–4‰ PDB, e.g., McCorkle et al., 1985; Patterson and Walter, 1994, also see Fig. 1), rxn. (3) adds dissolved inorganic carbon (DIC) to sediment pore waters that is relatively light (i.e., depleted in ^{13}C) as compared to bottom water values of ~0–2‰ (Zeebe and Wolf-Gladrow, 2001; also see Dill, 1991; Patterson and Walter, 1994). Furthermore, differences between the $\delta^{13}C$ of sediment organic matter and carbonates implies that the $\delta^{13}C$ of pore water DIC should provide information on the relative contributions of carbon to the pore water DIC pool from aerobic respiration and carbonate dissolution. Such analyses have been carried out successfully in both deep sea (e.g. Gehlen et al., 1999; Martin et al., 2000; McCorkle et al., 1985; Sayles and Curry, 1988) and continental margin (Presley and Kaplan, 1968) sediments. In contrast, in some shallow water marine environments the pore water DIC pool was found to be too enriched in ^{13}C and therefore could not be explained solely by these processes (Eldridge and Morse, 2000; McNichol et al., 1991).

In this paper, we present results of pore water DIC stable isotope studies in Great Bahamas Bank (GBB) sediments, which suggest that carbonate dissolution and reprecipitation both are important in shallow water carbonate sediments, and also influence the isotopic composition of pore water DIC. The significance of such a dissolution/reprecipitation process is examined with a simple closed-system model, and all of the results are used to re-assess the importance of carbonate reprecipitation in the early diagenesis of carbonate sediments.

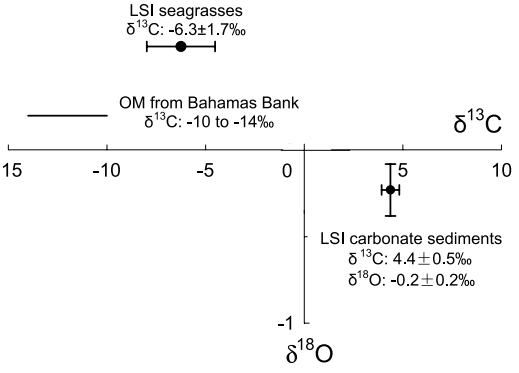

Fig. 1. $\delta^{13}C$ of carbonate sediments and seagrasses. Sedimentary organic matter $\delta^{13}C$ data are from the literature (Rasmussen et al., 1990; Scalan and Morgan, 1970).

2. Study area and methods

2.1. Sampling locations

Pore water, sediments and seagrass samples were collected at sampling locations around Lee Stocking Island (LSI), Exuma Cays, Bahamas (Fig. 2), using the Caribbean Marine Research Center (CMRC) as our base of operation. The majority of the results described here were obtained in May–June 2003 (LSI 7), although some results from our May–June 2002 trip (LSI 6) are also described. Additional details about LSI sediments are presented in Section 3.1.

2.2. Sample collection and processing

Pore waters were collected *in situ* by divers using sippers designed to collect pore waters from sandy sediments such as those around LSI (Burdige and Zimmerman, 2002). The sippers consist of a set of 10 ml Hamilton Gastight® syringes held in a rigid rack mounted on a small plate (6″ × 12″) with probes of different lengths (1–20 cm) that stick into the sediments. The syringes are attached to metal springs that when released, slowly pull back on the plunger and draw the sample into the syringe. In this study, the sampling probes consisted of 18 gauge (ID 1.024 mm) Luer-lock needles that were cut to the appropriate lengths, silver soldered at the bottom end, and then rounded. Eight sample holes (0.38 mm ID) were drilled into the tube 2 mm from the tip (see Berg and McGlathery, 2001 , for further details). The sampling probes are connected to the glass syringes with plastic three-way stopcocks, which allow the divers to seal the syringes *in situ* immediately after pore water collection. The pore water volume retrieved with these samplers was usually 8–10 ml per sample. Additional details about the design and use of these sediment sippers can be found in Burdige and Zimmerman (2002).

Pore water samples collected in this fashion were returned to the laboratory at CMRC for processing within 1 h of collection. First, dissolved O_2 was determined on unfiltered samples taken directly from the glass syringe (Burdige and Zimmerman, 2002; Hu and Burdige, unpubl. data). Next, samples were filtered (0.45 μm dia. nylon disc filters) into appropriate storage vessels for analysis either at CMRC or back at ODU (Table 1).

2.3. Analytical procedures

Total alkalinity was determined by Gran titration (Grasshoff et al., 1999) with automated end-point detection (uncertainty, ±2%) using a Cole-Parmer pH electrode and a Metrohm 785 DMP Titrino automatic titrator. The titrant was certified 0.02 N HCl, and Scripps Reference Seawater for CO_2 Measurement (Batch 51, 1999) was also used as an external reference standard (Dickson et al., 2003). Pore water DIC concentrations were determined coulometrically using a UIC Inc 5011 coulometer (DOE, 1994), with

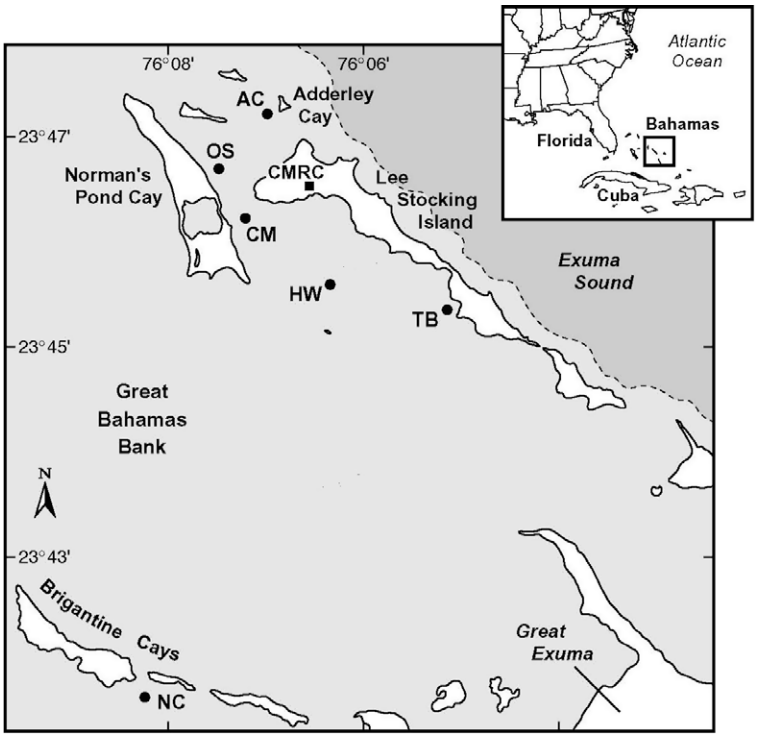

Fig. 2. A map of the LSI 6 and LSI 7 sampling sites.

Table 1
Sample storage and processing

Sample type	Sample storage	Time of analysis
DIC (concentration)	1.8 ml serum vials were filled completely and crimp-sealed with no headspace	Within 2 months (ODU)
DIC ($\delta^{13}C$)	Same as DIC (concentration)	Within 6 months (ODU)
Titration alkalinity	3 ml plastic syringe were partially filled with no headspace and sealed with three-way stopcocks	Within 2 days (Bahamas)
Sulfide	Same as DIC (concentration)	Within 2 days (Bahamas)
Major ions (Ca^{2+}, SO_4^{2-})	2 ml snap-cap vials were partially filled and sealed	Within 2–3 months (ODU)
Chlorinity	Same as major ions	Within 2–3 months (ODU)
Salinity	Measured by refractometer	During sample processing

an uncertainty of <2%. Pore water chlorinity was determined by potentiometric titration using $AgNO_3$ with automatic end-point detection (Grasshoff et al., 1999) using a Titrino™ titrator and a Metrohm® Ag-Titrode (Metrohm Ti Application Note No. T-1). The $AgNO_3$ titrant was standardized against IAPSO standard seawater. No significant chloride concentration variation (<1% of the average bottom water value of 571 mmol/kg) was observed in the upper 20 cm of sediment pore waters. Sulfate was measured by ion chromatography with an uncertainty of 4% (Burdige and Zimmerman, 2002), while sulfide was determined using the spectrophotometric method described in Cline (1969) with an uncertainty of ~2%.

The $\delta^{13}C$ of pore water DIC was determined by following the approach described in Salata et al. (2000). Briefly, 0.1 ml concentrated H_3PO_4 (75%) was first pipetted into 1.8 ml serum vials, and the vials were crimp-sealed with rubber serum stoppers and open top aluminum caps. The sealed vials were evacuated using a VacTorr™ 25 vacuum pump (Precision Scientific) for 3 min, and 0.8 ml of a pore water sample was then immediately injected into the vial using a 1 ml Hamilton Gastight® syringe flushed with ultra pure He. Fast effervescence was observed upon sample injection. After sample acidification, the vials were equilibrated to atmospheric pressure with ultrapure He using a flow controller equipped with a manometer (see Salata et al., 2000, for details). All acidified sample vials were placed on a shaker table and agitated for 5 h followed by headspace CO_2 isotopic analysis within 30 h of acidification. The headspace gas was extracted using a 100 µl Hamilton Gastight syringe after injecting ultra pure He into the sample vials to compensate for changes in the headspace pressure caused by sample removal. The CO_2 in the headspace gas was separated from water vapor by gas chromatography and the $\delta^{13}C$ of the CO_2 was measured on a PDZ Europa® GEO 20-20 isotopic ratio mass spectrometer

(IRMS) with a precision of 0.2‰. All samples were determined in duplicate by this procedure. The IRMS was calibrated using two different laboratory CO_2 gas standards.

Pore water DIC $\delta^{13}C$ values were calculated using the measured $\delta^{13}C$ of the headspace CO_2 corrected for the fractionation between the aqueous and gaseous phases. At 25 °C, the isotopic fractionation ($10^3 \ln\alpha$) for this exchange is 1.1‰ with the gaseous phase being enriched in ^{13}C (see Salata et al., 2000 and references therein). In preliminary studies examining this extraction procedure, we determined the $\delta^{13}C$ of the headspace CO_2 as a function of the time after acidification; within 5–30 h, the headspace gas reached equilibrium with the aqueous phase, and there was no apparent contamination or loss of headspace gas. The minimum equilibration time here (5 h) is significantly shorter than the 15 h in Salata et al. (2000), and indicates that agitation of the vials after acidification greatly enhances the rate of isotope exchange between the gaseous and aqueous phases.

Seagrass samples collected *in situ* by divers were separated into leaves and rhizome/root tissues, and first soaked for 30 min in 1 N HCl to remove any attached carbonate. This was followed by a distilled water rinse to remove excess acid. After oven drying at 60 °C, samples were ground into a powder (Craig, 1953; McMillan, 1980). High temperature combustion (HTC) in O_2 was used to convert organic carbon to CO_2 using an automated nitrogen/carbon (ANCA) elemental analyzer attached to the IRMS. Analytical uncertainty of these $\delta^{13}C$ measurements is 0.2‰. A subset of these samples were freeze dried at −20 °C *in vacuo* after acid cleaning and then ground to a powder; no significant differences were observed in measured seagrass $\delta^{13}C$ values between these two sample treatments. Both DIC and seagrass $\delta^{13}C$ values are reported relative to the PDB standard.

Isotopic analysis of sediment carbonate was carried out at the UC Davis Stable Isotope Lab. Dry sediments were first heated *in vacuo* at 75 °C for 30 min and the CO_2 gas used for analysis was generated by acidification of the treated sediments in a heated (90 °C) common acid bath (103% phosphoric acid). The resultant gas was then purified and introduced into a GVI Optima IRMS. The $\delta^{13}C$ values were calculated relative to V-PDB. Average precision (1σ) is ±0.04‰. Since the difference between V-PDB and PDB is negligibly small (Mook and de Vries, 2001), our complete isotopic data set is internally consistent.

Carbonate mineralogy of the sediments was determined by X-ray diffraction using a Philips PW 1729 X-ray diffractometer following the procedure of Morse et al. (1985). The scanning interval was 25° to 32°2′ 2θ at a scanning speed of 0.02° 2θ per 2 s scanning step. The calcite and aragonite standards used for calibration were both of marine origin. *Porites* was used for the aragonite standard and *Crassostrea* was used for the calcite standard. The peak area method was used to quantify the relative amounts of aragonite and high and low magnesian calcite (HMC and LMC) (Milliman and Bornhold, 1973; Morse et al., 1985). The mole percent Mg content in HMC was calculated from the shift of the major calcite peak (near 29.8° 2θ) using the lattice parameters in Goldsmith et al. (1961). The precision we observed in the XRD analysis of carbonate mineralogy was 1.5%, although the accuracy of this method is generally considered to be ~3–5% (Andrews, 1991; Milliman et al., 1993; Morse et al., 1985). The precision of the analysis of Mg content in HMC by XRD was 0.5%, and the XRD-determined Mg content of HMC agrees well with analyses using wet chemistry (Walter and Morse, 1984).

3. Results and discussion

3.1. Results and general trends in the data

Sites around LSI include unvegetated, well-sorted oolitic sands and seagrass meadows (mostly *Thalassia testudinum* or turtlegrass) of densities exceeding 500 shoots/m^2 (see below and discussions in Dill, 1991). Water depths range from ~2–10 m. Sediments in this area have a mean grain size of 200–750 μm (Stephens et al., 2003) and are comprised of biogenic calcareous skeletal debris, ooids, peloids and grapestones. The dominant minerals are aragonite (70–90 wt%) and high-Mg calcite (10–30 wt%) with a small amount of low-Mg calcite (generally <3–4 wt% of the bulk sediments). The Mg content of the HMC was consistently ~12 mol% (Table 2).

In this study, we divided the sampling sites into three groups based on seagrass densities (Bodensteiner and Zimmerman, unpubl. data; see Burdige and Zimmerman, 2002, for a description of the methods used here). Dense seagrass sites (sites AC, CM and NC) have average shoot densities of 561 ± 50 shoots/m^2 and LAI (leaf area index) values of 1.4 ± 0.1 (note that LAI is defined as m^2-one sided leaf area per m^2-seafloor, e.g. Campbell and Norman, 1998). Intermediate density seagrass sites (sites HW and TB) have average shoot densities of 274 ± 30 shoots/m^2 and average LAI values of 0.5 ± 0.2. Finally, bare oolitic sands (site OS) have no seagrass (shoot density and LAI equal to zero).

At all sites examined, DIC concentrations increase with sediment depth in the upper 20 cm (Fig. 3 and Table 3) and the magnitude of this increase is greatest at dense seagrass (DG) sites and smallest in the bare oolitic sands (OS). Intermediate density seagrass (IG) sites fall in-between the DG and OS sites, although they are closer in magnitude to the OS sites than the DG sites. These DIC concentration profiles in the seagrass vegetated sediments, along with alkalinity, Ca^{2+}, sulfate and O_2 profiles from LSI sediments (Hu and Burdige, unpubl. data) indicate that sediment carbonate dissolution occurs in the upper ~20 cm of these sediments largely as a result of aerobic respiration sustained by seagrass O_2 input (or pumping) into this portion of the sediments (also see similar pore water profiles and discussions in Burdige and Zimmerman, 2002). Consistent with this interpretation, more recent observations (Hu and Burdige, unpubl. data) indicate that >99% of the

Table 2
Sample site mineralogy (unit: wt% for mineralogy) [a]

Station		Aragonite	HMC	LMC	mol% Mg in HMC
DG	AC	57.0 ± 2.4	39.0 ± 1.7	4.0 ± 0.6	12.3 ± 0.03
	CM	63.1 ± 4.8	34.0 ± 4.2	2.9 ± 0.5	12.3 ± 0.1
	NC	81.4 ± 2.4	16.6 ± 2.4	2.0 ± 0.2	11.8 ± 0.03
IG	HW	83.8 ± 2.6	15.1 ± 2.4	1.1 ± 0.2	12.4 ± 0.1
	TB	84.2 ± 0.2	14.2 ± 0.1	1.6 ± 0.1	12.4 ± 0.5
OS	OS	84.6 ± 2.6	14.1 ± 2.8	1.3 ± 0.1	13.4 ± 0.2

[a] At each station, samples from three depths were analyzed (a surface sample in the upper 5 cm of sediment, a mid-depth sample near 10 cm, and a deep sample, generally at 16–20 cm depth). The values reported here for each station are averages and the uncertainties are standard deviations based on these three analyses.

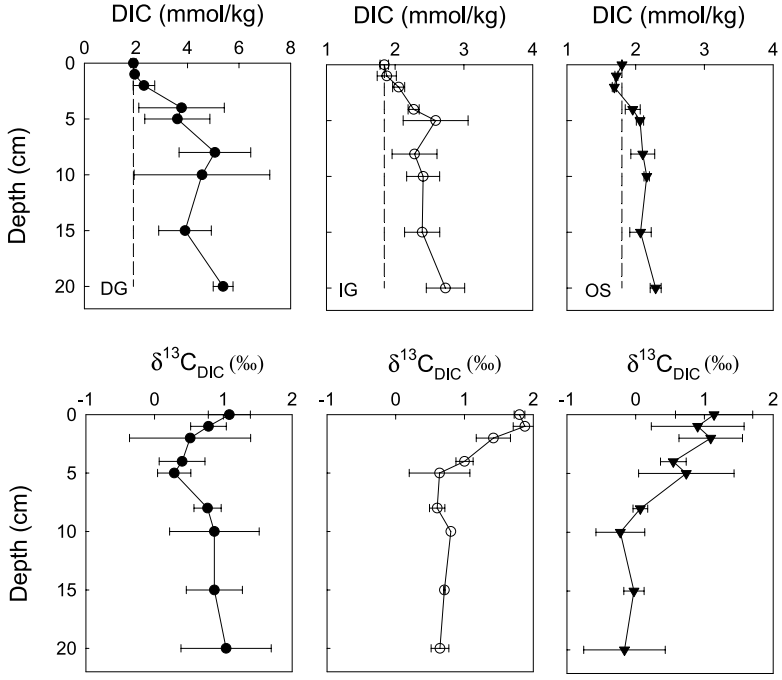

Fig. 3. Pore water depth profiles of DIC and the $\delta^{13}C$ of the DIC in dense and intermediate density seagrass sediments (DG and IG, respectively) and bare oolitic sand (no seagrasses, OS). The profiles shown here for each sediment type are average profiles based on individual profiles collected at different sites ($n = 4$, 2, and 2 profiles for DG, IG and OS sites; respectively; see Table 3). In the upper DIC concentration profiles, the dashed line indicates the bottom water concentration.

belowground seagrass biomass was distributed in the upper 20 cm of sediments.

At both the OS and IG sites, pore water DIC-$\delta^{13}C$ values decrease with sediment depth and reach constant values below ~10 cm (Fig. 3). However, the asymptotic $\delta^{13}C$ values at the OS site are slightly lighter than they are at the IG sites (approximately −0.1‰ versus 0.7‰). In contrast, while pore water DIC-$\delta^{13}C$ values at the DG sites also initially decrease with depth, they then show a mid-depth minimum at ~5 cm, and return to near-bottom water values (~1‰) by a sediment depth of 20 cm.

3.2. Sources of pore water DIC

The isotopic composition of sediment carbonate and organic matter in Bahamas Bank sediments is shown in Fig. 1 and Table 4. Note that the $\delta^{13}C$ of organic matter in these sediments is heavier than "typical" marine organic matter (approximately −20‰) most likely due to the input of seagrass-derived organic matter (Rasmussen et al., 1990). Seagrass organic matter is relatively heavy (e.g., LSI seagrasses are approximately −6‰) because their photosynthetic carbon uptake shows less discrimination against heavy carbon than "typical" marine phytoplankton, despite the fact that seagrasses are also C_3 type plants (Anderson and Fourqurean, 2003; Hemminga and Duarte, 2000).

Both sediment organic matter remineralization and sediment carbonate dissolution may contribute DIC to the pore water pool. Given the distinct differences in the carbon isotope composition of these two sources (Fig. 1), the $\delta^{13}C$ of pore water DIC can be used to estimate the rel-

Table 3
Pore water data for LSI 6 and LSI 7 sampling trips

Sites	Trip	Depth (cm)	pH	Cl^- (mmol/kg)	DIC (mmol/kg)	$\delta^{13}C$ (‰)	Alk (meq/kg)	Ca^{2+} (mmol/kg)	SO_4^{2-} (mmol/kg)	H_2S (mmol/kg)
DG										
AC	LSI7	0	8.03	588	1.84	1.41	2.00	10.93	28.5	0.00
		1	8.08	586	1.99	0.54	1.98	10.95	28.7	0.00
		2	7.52	581	2.65	0.37	2.64	10.89	26.7	0.00
		4	7.58	585	2.45	0.25	2.42	11.08	29.5	0.00
		5	7.41	580	2.63	0.15	2.84	11.48	27.5	0.38
		8	7.31	578	4.38	1.01	4.49	11.75	27.1	0.39
		10	7.50	568	2.32	0.44	2.39	11.22	23.3	0.93
		15	7.36	573	3.37	0.30	3.60	11.36	27.8	0.24
		20	7.31	576	5.13	1.01	5.33	11.80	29.2	1.29
CM	LSI7	0	7.95	597	2.03	1.04	1.95	10.80	30.6	—
		1	7.96	597	1.91	1.06	1.89	10.68	29.5	—
		2	8.01	594	1.88	1.59	1.80	10.91	30.7	—
		4	7.39	596	3.50	0.89	3.25	11.25	30.7	—
		5	7.34	591	5.04	0.01	2.97	11.75	30.5	—
		8	7.17	586	5.94	0.66	5.99	11.99	28.6	—
		10	7.36	582	3.95	0.48	3.73	11.38	31.1	—
		15	7.34	586	5.43	1.22	5.50	11.69	31.2	—
		20	7.29	583	5.94	1.59	5.96	11.65	30.2	—
CM	LSI6	0	8.08	576	1.95	0.69	2.29	10.74	29.7	—
		1	8.03	569	1.96	0.76	2.40	10.68	30.3	—
		2	7.96	571	2.03	0.66	2.33	10.66	30.4	—
		4	7.28	581	6.17	0.31	6.73	12.12	29.3	—
		5	7.03	584	4.29	0.47	4.13	11.44	30.5	—
		8	7.16	582	6.47	0.84	7.11	12.54	29.6	—
		10	7.09	586	8.37	1.83	8.73	12.84	29.6	—
		15	7.37	588	3.38	0.87	3.62	11.35	31.0	—
		20	7.19	586	5.11	1.43	5.44	11.93	30.7	—
NC	LSI7	0	7.89	581	1.80	1.21	2.06	10.74	29.4	0.00
		2	7.59	594	2.70	-0.55	3.02	11.10	28.9	0.01
		4	7.41	589	2.96	0.16	2.75	10.96	30.2	0.01
		5	7.44	588	2.47	0.50	2.43	10.77	29.4	0.60
		8	7.43	595	3.46	0.57	3.55	11.37	29.0	0.08
		10	7.41	588	3.62	0.72	3.62	11.25	28.5	0.00
		15	7.40	594	3.44	1.09	3.46	11.28	27.3	1.12
		20	7.38	596	5.35	0.12	5.15	11.64	28.9	0.77
IG										
HW	LSI7	0	7.80	577	1.88	1.88	2.13	10.60	—	—
		1	7.90	579	2.04	2.05	2.18	10.73	—	—
		2	7.75	584	1.97	1.67	2.08	10.75	—	—
		4	7.45	593	2.24	0.88	2.06	10.67	—	—
		5	7.34	593	3.11	0.20	3.22	11.02	—	—
		8	7.28	590	2.63	0.49	2.61	10.96	—	—
		15	7.38	588	2.68	0.71	2.73	10.92	—	—
		20	7.47	590	2.41	0.58	1.77	10.94	—	—
TB	LSI7	0	8.01	590	1.77	1.72	2.01	11.02	29.4	0.01
		1	7.98	590	1.81	1.71	1.97	10.96	28.0	0.01
		2	7.73	594	2.04	1.17	2.29	10.89	29.1	0.01
		4	7.54	591	2.21	1.13	2.04	10.82	29.4	0.01
		5	7.54	591	2.19	1.08	2.29	10.83	29.1	0.01
		8	7.51	592	2.23	0.72	2.24	10.74	29.2	0.01
		10	7.46	593	2.65	0.80	2.80	10.43	29.5	—
		15	7.49	594	2.19	0.70	2.14	11.22	29.6	0.02
		20	7.39	589	2.90	0.71	2.89	10.78	28.7	0.04
OS										
OS	LSI7	0	8.10	591	1.74	1.70	2.03	10.52	29.27	—
		1	7.94	593	1.66	1.58	1.95	10.71	28.64	—
		2	7.93	588	2.07	1.55	1.91	—	—	—
		4	7.56	582	2.01	0.36	2.18	10.64	28.91	—
		5	7.59	583	2.28	1.43	2.06	—	—	—
		8	7.59	584	2.20	−0.04	2.21	10.62	28.43	—

Table 3 (*continued*)

Sites	Trip	Depth (cm)	pH	Cl^- (mmol/kg)	DIC (mmol/kg)	$\delta^{13}C$ (‰)	Alk (meq/kg)	Ca^{2+} (mmol/kg)	SO_4^{2-} (mmol/kg)	H_2S (mmol/kg)
		10	7.64	583	2.23	−0.58	2.22	10.55	28.40	—
		15	7.60	582	2.21	0.12	2.19	10.69	28.32	—
		20	7.64	584	1.74	−0.76	2.28	10.77	27.78	—
OS	LSI6	0	7.57	632	1.80	0.58	1.92	11.43	32.3	—
		1	8.06	621	1.70	0.23	2.12	11.43	31.5	—
		2	8.08	613	1.72	0.63	2.20	11.21	31.7	—
		4	7.81	621	1.85	0.74	2.12	11.84	31.1	—
		5	7.73	590	2.12	0.04	2.43	11.09	30.1	—
		8	7.88	601	1.93	0.18	2.26	11.22	33.3	—
		10	7.79	599	2.12	0.13	2.42	11.03	30.8	—
		15	7.84	615	1.91	−0.17	2.25	11.20	31.7	—
		20	7.80	599	2.37	0.43	2.60	10.81	30.4	—

Table 4
Isotopic composition of seagrass and sedimentary carbonates (units: ‰ PDB)

	DG	IG	OS
Seagrass[a]	-7.8 ± 0.2	-4.5 ± 0.2	—
Sediments	4.0 ± 0.1	4.6 ± 0.2	5.0 ± 0.03

[a] There is no significant difference among isotopic values of seagrass leaves and rhizome/root tissues. Thus average values are reported here.

ative contribution of these two sources to the pore water DIC pool. The approach we have taken here is based on that presented by Sayles and Curry (1988) and Martin et al. (2000) in which they show that plots of $(\delta^{13}C\text{-DIC})\cdot[DIC]$ versus [DIC] are generally linear, and that the slope of such plots is the $\delta^{13}C$ of the DIC being added to the pore waters (defined here as $\delta^{13}C_{added}$; Fig. 4). Although not explicitly discussed in these works, this approach is very similar to that used to examine elemental ratios of the organic matter undergoing remineralization in marine sediments using pore water property–property plots (Berner, 1977; Burdige, 2006). However in the approach taken here, if we assume that total [DIC] is roughly equal to the pore water concentration of $DI^{12}C$ and that $(\delta^{13}C\text{-DIC})\cdot[DIC]$ is a "proxy" for $DI^{13}C$, then the slope of this line will yield the carbon isotopic composition of the DIC being added to the pore waters (see the Appendix for a more rigorous derivation).

Transport processes such as pore water advection or diffusion generally can impact the ability to use such property–property plots to examine these aspects of diagenetic processes in marine sediments (also see Hammond et al., 1999, for further details). For example, given the estimated permeability of LSI sediments (Burdige and Zimmerman, 2002), pore water advection through the sediments, due to near seabed pressure gradients caused by surface roughness or biogenic structures, is thought to be a significant transport process down to a depth of at least several centimeters (Huettel and Webster, 2001). This type of advection clearly affects concentrations of pore water solutes such as DIC and alkalinity, along with the ability to estimate rates of sediment processes from such pore water data without an accurate estimate of the magnitude of this advection. However, in terms of calculations such as those illustrated

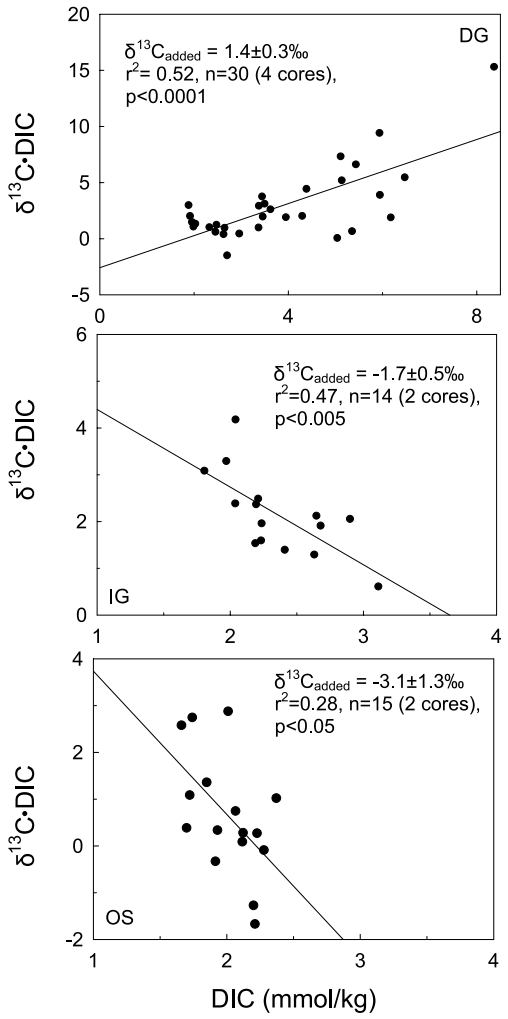

Fig. 4. Plot of $(\delta^{13}C\text{-DIC})\cdot[DIC]$ (or $\delta^{13}C\cdot DIC$) versus DIC for the three sediment types studied here. As discussed in the text, the slope of this line is the $\delta^{13}C$ of the DIC added to the pore waters ($\delta^{13}C_{added}$). Note the different axis scales on each figure.

in Fig. 4, pore water concentrations will simply move "along" the mixing lines shown here as a function of pore water advection and DIC addition without changing the slope of the line (i.e., $\delta^{13}C_{added}$ will be largely independent of pore water advection).

Diffusion can also affect the interpretation of these property–property plots, although in most cases these effects are easily accounted for (Berner, 1980; Burdige, 2006). However, in the specific calculations presented here, the effects of diffusion may be slightly more complicated than that discussed in these references; nevertheless, as we will show in the next section, we do not believe that this significantly compromises the interpretation of the plots in Fig. 4.

Fits to our pore water data using this approach are shown in Fig. 4 and summarized in Table 5. Interpretation of these results in terms of rxns. (1)–(3) and possible sources of DIC to the pore waters requires that we make several assumptions. The first is that these sediments become sufficiently undersaturated below the sediment–water interface such that the coupling of rxns. (1)–(3) describes the processes that affect downcore variations in alkalinity, DIC and Ca^{2+} in these sediments. Evidence for this can be seen in Fig. 5 where we see the tight co-variance between increases in pore water alkalinity and DIC, consistent with these equations; similar trends are also seen with increases in pore water Ca^{2+} and DIC (results not shown here, but see Burdige and Zimmerman, 2002, for related discussions and plots).

Another important assumption is that there is no net sulfate reduction in these sediments, since this process produces alkalinity and DIC at roughly equimolar ratios in the absence of carbonate dissolution, as shown by the following reaction,

$$2CH_2O + SO_4^{2-} \rightarrow H_2S + 2HCO_3^- \quad (4)$$

Several lines of evidence are consistent with the lack of net sulfate reduction occurring in these sediments (also see related discussions in Section 3.2.1). Our previous work (Burdige and Zimmerman, 2002), along with observations in this study (Fig. 6), demonstrate that pore water sulfate concentrations do not vary with sediment depth down to 20 cm, and show no consistent downcore trends relative to bottom water values. In contrast, depth profiles of alkalinity, DIC and Ca^{2+} increase "relatively" smoothly (and consistently) with depth (Fig. 3; Burdige and Zimmerman, 2002; Hu and Burdige, unpubl. data). Finally, a property-property plot of ΔSO_4^{2-} versus ΔAlkalinity (not shown here) has a slope that is indistinguishable from 0, and not the value of approximately −0.5 predicted by rxn. (4).

Given these observations, if we assume that contributions of DIC to the pore waters come from organic carbon

Table 5
Isotopic composition of the DIC added to sediment pore waters

	DG	IG	OS
$\delta^{13}C_{added}$ [a] (‰)	1.4 ± 0.3	−1.7 ± 0.5	−3.1 ± 1.3
$\delta^{13}C_{OM}$ [b] (‰)	−1.2 ± 0.5	−8.0 ± 1.0	−11.1 ± 2.6

[a] From Fig. 4, the uncertainties shown here are standard errors of the linear regressions in this figure.
[b] The calculated $\delta^{13}C$ of the sediment organic matter undergoing remineralization (see Eq. (5) and associated discussions in the text).

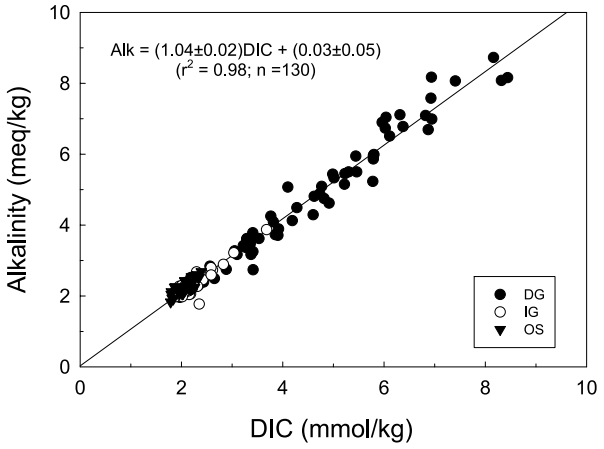

Fig. 5. Measured pore water alkalinity versus DIC in LSI sediments. The linear regression shown here was carried out using the data from sediment depths >2 cm (see discussions in Burdige and Zimmerman, 2002 for details).

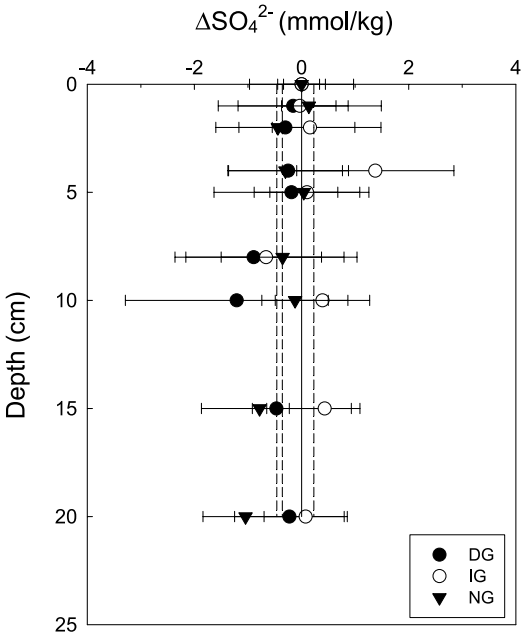

Fig. 6. Depth profiles of pore water ΔSO_4^{2-}, where $\Delta SO_4^{2-} = [SO_4^{2-}]_{pw} - ([SO_4^{2-}]_{bw}/[Cl^-]_{bw}) \cdot [Cl^-]_{pw}$ (subscripts pw and bw represent pore water and bottom water, respectively). This approach allows us to differentiate between small changes in sulfate concentration due to net sulfate reduction and those associated with change in pore water salinity. The dashed lines represent the average ΔSO_4^{2-} values in the DG, IG and OS sediments (−0.5 ± 0.4, 0.2 ± 0.6 and −0.4 ± 0.4 mmol/kg, respectively, versus 0 ± 1.1 mmol/kg for bottom water samples). Similar results were obtained in these sediments by Burdige and Zimmerman (2002), and indicate that minimal net sulfate reduction occurs in these sediments.

oxidation and carbonate dissolution, then the following mass balance should be valid:

$$\delta^{13}C_{added} = f_{OM} \times \delta^{13}C_{OM} + f_C \times \delta^{13}C_C \quad (5)$$

where f is the fraction of DIC input from either organic carbon oxidation (subscript OM) or carbonate dissolution (subscript C). Furthermore, if the rate of carbonate dissolution is fast relative to organic matter oxidation, i.e., rxns. (1)–(3) are tightly coupled (Martin and Sayles, 2003), then $f_{OM} = f_C = 0.5$. With these assumptions then, we can calculate the $\delta^{13}C$ of the organic matter undergoing remineralization ($\delta^{13}C_{OM}$) based on the values of $\delta^{13}C_C$ from Table 4 and $\delta^{13}C_{added}$ from Table 5. These results are also shown in Table 5.

In the bare oolitic sands (OS site), the calculated $\delta^{13}C_{OM}$ value ($-11.1 \pm 2.6‰$) agrees well with the results from past studies of the $\delta^{13}C$ of organic matter in Bahamian sediments (approximately $-10‰$ to $-14‰$; Rasmussen et al., 1990; Scalan and Morgan, 1970). Furthermore, if we assume that water column particulate organic matter and/or benthic algal production has $\delta^{13}C$ values that are in the range of $-17‰$ to $-23‰$ (e.g., Craig, 1953; Eadie and Jeffrey, 1973), this result suggests that the organic matter being remineralized in such bare sands is a mixture of non-seagrass derived organic matter and exported seagrass litter (with a presumed $\delta^{13}C$ value between $-4‰$ and $-8‰$; see Fig. 1).

In sediments underlying intermediate density seagrass beds (IG sites), the calculated value of $\delta^{13}C_{OM}$ ($-8.0 \pm 1.0‰$) is consistent with the range of $\delta^{13}C$ values for LSI seagrasses (see Fig. 1). This suggests that seagrass-derived organic matter represents the major type of organic matter undergoing remineralization here. However, the $\delta^{13}C$ of seagrasses at the IG sites ($-4.5 \pm 0.2‰$) is heavier than this value of $\delta^{13}C_{OM}$, suggesting that some fraction of the organic mater undergoing remineralization in the IG sediments could be either more typical detrital marine organic matter (as above), or lighter, exported seagrass litter from other nearby seagrass meadows (e.g., the DG sites; see Table 4).

In their studies of tropical seagrass sediments in coastal Thailand, Holmer et al. (2001) observed that sediment bacterial biomass (based on the analysis of bacteria specific polar lipid derived fatty acids) had $\delta^{13}C$ values that are very close to that of the seagrasses found at their site (ca. $-12‰$), despite the existence of much lighter bulk sedimentary organic carbon (ca. $-22‰$), which is presumably detrital material of algal origin. Taking all of these observations together, we believe that organic matter remineralization in these IG sediments is largely driven by seagrass-derived organic matter, despite the fact that the presence of seagrasses (specifically the overlying leaf canopy) dampens water motion and promotes the deposition of inorganic and organic (detrital) particles from the water column to the sediments (e.g., Hemminga and Duarte, 2000; Koch and Gust, 1999). The remineralization of seagrass-derived materials in these sediments (as well as those at the DG sites) may occur through the incorporation of reactive seagrass litter into the bulk sediment organic matter pool, or through the release of seagrass-produced DOM from the roots and rhizomes of actively growing plants (Holmer et al., 2001).

3.2.1. Sources of DIC in the pore waters of dense seagrass sediments

At the OS and IG sites, pore water DIC isotopic mass balance appears to be satisfactorily explained by rxns. (1)–(3) given the likely sources of organic matter to these sediments. In contrast, the calculated $\delta^{13}C_{OM}$ in the dense seagrass sediments (DG sites) appears to be problematic ($\delta^{13}C_{OM} = -1.2 \pm 0.5‰$), since we know of no such heavy organic carbon in marine sediments that may be of biological origin. To the best of our knowledge, seagrasses have the heaviest organic carbon that is produced in shallow marine environment, with $\delta^{13}C$ values of up to $-3‰$ (Hemminga and Mateo, 1996). Furthermore, seagrasses collected at the DG sites were in fact much lighter ($-7.8 \pm 0.2‰$).

These observations at the DG sites are not unique to these sediments, since other workers (Eldridge and Morse, 2000; McNichol et al., 1991) have similarly observed ^{13}C-enriched pore water DIC in coastal sediments that differ greatly from each other and from our DG sites (temperate, bioirrigated sediments in Buzzards Bay, MA, and highly sulfidic seagrass sediments in the negative estuary Laguna Madre, TX). One possible mechanism for this isotopic enrichment may involve the preferential diffusion of isotopically heavy bottom water carbonate ion into the sediments (McNichol et al., 1991). This can occur because DIC and alkalinity are composed of several chemical species (e.g., carbonate and bicarbonate ions, as well as aqueous CO_2 [DIC only]), and changes in alkalinity and DIC with sediment depth can then lead to differing changes in dissolved carbonate and bicarbonate concentrations, and hence differential fluxes of these dissolved constituents across the sediment–water interface.

In particular, bottom waters at LSI are supersaturated with respect to all carbonate mineral phases present in the sediments (Burdige and Zimmerman, 2002), and for example, our calculations for LSI 6 and 7 indicate that the average bottom water saturation state with respect to aragonite ($\Omega_{aragonite}$), the dominant carbonate mineral in these sediments, is ~2.2. Therefore metabolic acid produced by aerobic respiration (rxn. 1) is first neutralized by reacting with dissolved carbonate producing bicarbonate according to:

$$CO_2 + H_2O + CO_3^{2-} \rightarrow 2HCO_3^- \quad (6)$$

The consumption of CO_3^{2-} by this reaction lowers the saturation state of the pore water, and once the pore waters become sufficiently undersaturated, dissolution of the most soluble carbonate mineral occurs according to the coupled rxns. (1)–(3). This also results in a carbonate ion gradient across the sediment–water interface (Fig. 7), and bottom water carbonate can diffuse into the sediments despite the fact that there is a net flux of alkalinity and DIC (mainly

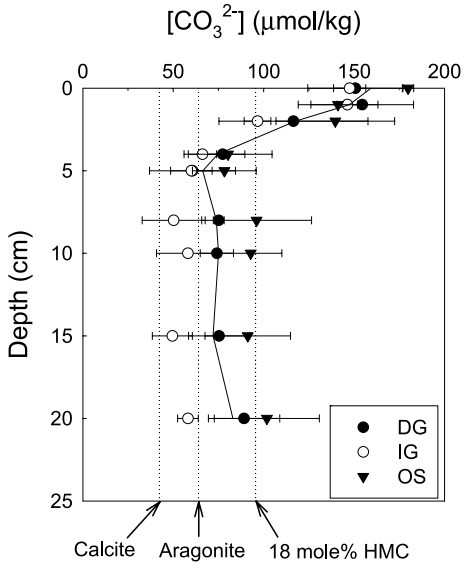

Fig. 7. Calculated carbonate ion concentrations in LSI sediments, determined using the program CO2SYS (Lewis and Wallace, 1998). The curve represents the average depth profile for pore water carbonate concentration in all three sediment types. The three arrows at the bottom of the figure represent the saturation carbonate ion concentrations for 18 mol% HMC, aragonite and calcite. These concentrations were calculated using average pore water [Ca^{2+}] (Hu and Burdige, unpubl. data), [Mg^{2+}] calculated from chlorinity data, solubility constants for each mineral phase at 25 °C (Mucci, 1983; Walter and Morse, 1984), and an average pore water salinity of 37.

in the form of bicarbonate) out of the sediments (also see similar discussions in Cai et al., 2000). Furthermore, because bottom water DIC is generally isotopically heavier than pore water DIC just below the sediment–water interface (e.g., see Fig. 2), this process may potentially lead to the enhanced diffusion of ^{13}C-enriched carbonate ion into the sediments.

In spite of these general trends, we do not feel that this process can significantly contribute to the heavy value of $\delta^{13}C_{added}$ seen in the DG sediments. First, an examination of Fig. 7 indicates that depth profiles of carbonate ion are roughly similar at all sites. It is thus unlikely that the diffusion of isotopically heavy carbonate ion is significant only in DG sediments (however, we also note that a more rigorous examination of this problem requires an isotope-specific, reactive-transport model; e.g., Gehlen et al., 1999). Furthermore, the shape of the pore water $\delta^{13}C$-DIC profile at the DG sites (Fig. 3) also argues against a water column source for this heavy DIC, since the apparent input here of heavy DIC into the pore waters does not occur at the sediment–water interface but at sediment depths below ~5 cm. Finally, we also note that [CO_3^{2-}] is essentially invariant below sediment depths of ~5 cm (Fig. 7, also see Burdige and Zimmerman, 2002). This implies that alkalinity and DIC production must be tightly coupled at these sediment depths, because at the pH values of these sediments [CO_3^{2-}] ≈ Alkalinity–DIC, and if $\Delta[CO_3^{2-}] \approx 0$ then ΔAlkalinity ≈ ΔDIC. Again, this can only occur if carbonate dissolution is tightly coupled to aerobic respiration through rxns. (1)–(3), and the neutralization of metabolic CO_2 by downwardly diffusing carbonate ion is of minor importance.

Another possible explanation of the observation that ^{13}C-enriched DIC is added to the pore water at the DG sites is that the reaction stoichiometry described above for metabolic carbonate dissolution (rxns. (1)–(3)) is not valid in the DG sediments, and that in fact $f_C > f_{OM} \neq 0.5$. This then requires an additional acid source to dissolve sediment carbonate, in addition to the isotopically light metabolic CO_2. One possible mechanism by which this acid may be generated is through sulfide oxidation, either of dissolved sulfide or particulate sulfides such as iron monosulfide (FeS). While this possibility has been discussed by other workers (Ku et al., 1999; McNichol et al., 1991), there are several reasons why we believe that this is not likely important in LSI sediments.

In our sediments, and the Florida Bay sediments examined by Ku et al. (1999), net sulfate reduction appears to be minimal based, in part, on the lack of detectable pore water sulfate gradients (see Fig. 6 and Burdige and Zimmerman, 2002). At the same time though, oxygen and sulfur stable isotope measurements in Florida Bay sediments (Ku et al., 1999) and pore water sulfide measurements in LSI sediments (Fig. 8) both indicate that there is some amount of gross sulfate reduction in both of these sediments. As a result, there is a tight coupling between sulfate reduction and sulfide oxidation in these sediments. In LSI sediments, this coupling is largely mediated by the fact that seagrass O_2 input occurs down to depths of ~10–20 cm, overlapping with depths where pore water sulfide data suggest sulfate reduction occurs. Furthermore, as Burdige and Zimmerman (2002) note, such a coupling between sulfate reduction (and its resulting bicarbonate production) and sulfide oxidation (and its resulting proton production) simply results in the net production of H_2CO_3 (aqueous CO_2). Thus from the standpoint of the carbonate system and sediment car-

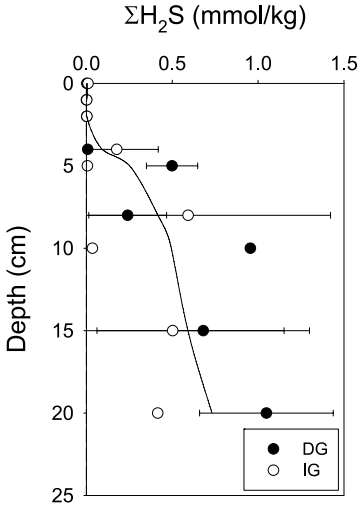

Fig. 8. Pore water depth profiles of total dissolved sulfide ($\sum H_2S$) in dense and intermediate density seagrass sediments.

bonate dissolution, this is identical to that which occurs from aerobic respiration of sediment organic matter (rxn. 1).

In some coastal sediments however, there is net sulfate reduction that occurs during some portions of the year involving seasonal storage of sulfide minerals during spring/summer. This is then followed by sulfide oxidation during fall/winter. This leads to a temporal uncoupling of sulfate reduction and sulfide oxidation, which then results in seasonal variability of sediment carbonate mineral saturation state (supersaturated during spring/summer and undersaturated in fall/winter; Green and Aller, 1998, 2001; also see Sampou and Oviatt, 1991). However, several lines of evidence argue against this being an important process in LSI sediments, including the lack of seasonality in biogeochemical processes occurring in these sediments versus that observed in temperate terrigenous sediments (e.g., Burdige and Zimmerman, 2002). The lack of significant Fe in carbonate sediments such as these (e.g., Morse et al., 1985) also minimizes the ability to sequester any dissolved sulfide that is produced in these sediments as iron sulfides.

Finally, it is important to recognize that closed system calculations (Boudreau and Canfield, 1993; Stoessell, 1992) do indicate that small amounts of net sulfate reduction (~0.7 mM sulfate depletion) can lead to undersaturation with respect to either aragonite or some forms of high-Mg calcite (Walter and Morse, 1984). This amount of sulfate reduction may be within the uncertainty of our sulfate measurements, and it could represent another mechanism by which sediment organic matter remineralization processes may be coupled to carbonate dissolution. However, open-system calculations (which allow for transport processes such as diffusion) suggest that the occurrence of this undersaturation during small amounts of sulfate reduction is unlikely in most marine sediments (Boudreau and Canfield, 1993). Furthermore, because H_2S likely contributes only one proton towards carbonate dissolution at pH values of typical marine sediments, the coupling of sulfate reduction and carbonate dissolution may be approximately expressed as,

$$SO_4^{2-} + 2CH_2O + CaCO_3 \rightarrow Ca^{2+} + HS^- + 3HCO_3^- \quad (7)$$

implying here that $f_{OM} \approx 0.67$ and $f_C \approx 0.33$. Since the resolution of the question of an extra acid source in DG sediments requires $f_C > f_{OM}$, the occurrence of rnx. (7), if indeed it occurs in an open sediment system, does not provide an explanation for the heavy value of $\delta^{13}C_{added}$ seen in the DG sediments.

3.2.2. Heavy values of $\delta^{13}C_{added}$ in DG sediments as a result of carbonate mineral reprecipitation

Given the difficulties in explaining the ^{13}C enrichment of DIC in dense seagrass sediment pore waters by any of the above-discussed mechanisms, we propose that a coupling of carbonate dissolution and reprecipitation may actually explain these observations. A conceptual model for how this might occur is shown in Fig. 9. This somewhat oversimplified view of carbonate mineral diagenesis in these sediments recognizes that because of differences in the solubility of carbonate phases in these sediments (calcite, aragonite and HMC), pore waters which are undersaturated with respect to one or more metastable phases (e.g., HMC) are still supersaturated with respect to calcite (or low-Mg calcite; e.g., see Fig. 7). Thus, in these sediments there may be net dissolution of a more soluble carbonate phase along with reprecipitation of a more stable phase. Note that a further discussion of the phases that may actually be dissolving and reprecipitating in these sediments will be presented at the end of Section 3.3.

Evidence for the occurrence of such coupled dissolution/reprecipitation processes has indeed been observed in many natural systems. Groundwater studies (Gonifiantini and Zuppi, 2003; Plummer and Sprinkle, 2001) have demonstrated that due to small Gibbs free energy differences, impure/less stable carbonate phases (analogous to HMC in our sediments) tend to dissolve and re-crystallize to form purer calcite phases. Evidence for carbonate dissolution/reprecipitation in Florida Bay and Bahamas Bank sediments have also been presented, using stable isotope, trace element and microscopic observations (Hover et al., 2001; Patterson and Walter, 1994; Rude and Aller, 1991; Walter et al., 1993). A study carried out by Walter et al. (2006) in these sediments has also shown that an apparent isotope exchange enriches the pore water DIC pool with ^{13}C through carbonate reprecipitation.

Based on the above discussion, we suggest that net dissolution of a metastable carbonate phase such as HMC occurs in DG sediments through metabolic CO_2 production from the remineralization of seagrass-derived organic

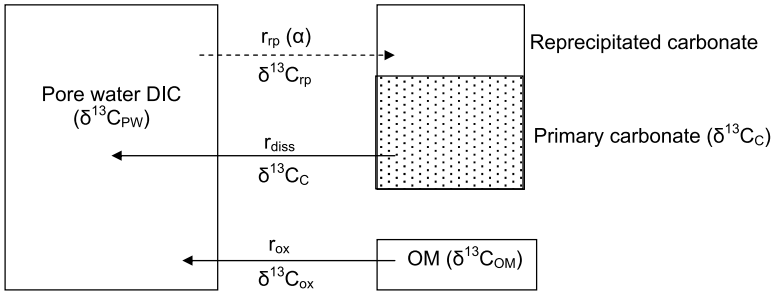

Fig. 9. A schematic illustration of the dissolution/reprecipitation mechanism discussed in the text, and its impact on the $\delta^{13}C$ of pore water DIC.

matter (as in the IG sediments); this process is ultimately driven by the fact that sediment pore waters become undersaturated with respect to HMC just below the sediment–water interface. However, because the pore waters also remain supersaturated with respect to more stable carbonate phases, (e.g., calcite, see Fig. 7), there is a component of this gross dissolution that is balanced by the reprecipitation of one or more of these stable carbonate phases. This secondary carbonate phase presumably forms under chemical/isotopic equilibrium with respect to the pore water DIC.

This model for carbonate diagenesis then implies that the pore water DIC pool is more than a simple "reservoir" for the end-products of organic matter remineralization and carbonate dissolution. Rather, the pore waters also serve as an intermediate through which sedimentary carbonates cycle during dissolution/reprecipitation. As we will see below, recycling of the sedimentary carbonate through the pore water DIC pool has a dramatic effect on the (now) "apparent" $\delta^{13}C$ of the DIC being added to the pore waters. Furthermore, the net addition of light DIC from organic matter oxidation to the pore water DIC pool also implies that the secondary carbonate phase that forms will be isotopically lighter than the primary sediment carbonate (also see Walter et al., 2006).

To examine these processes more quantitatively, we will use a closed system model based on Fig. 9. In this model pore water DIC is affected by three processes: organic matter oxidation, carbonate dissolution and secondary carbonate reprecipitation. Changes in the concentration $DI^{12}C$ and $DI^{13}C$ are then given by

$$\frac{d[DI^{13}C]}{dt} = r_{diss} \times F_{sed} + r_{ox} \times F_{OM} - r_{rp} \times F_{rp} \quad (8)$$

$$\frac{d[DI^{12}C]}{dt} = r_{diss} \times (1 - F_{sed}) + r_{ox} \times (1 - F_{OM}) - r_{rp} \times (1 - F_{rp}) \quad (9)$$

where F_i is the isotopic abundance of ^{13}C in the original carbonate sediments (subscript sed), the sedimentary organic matter (subscript OM) and the secondary carbonate (subscript rp); r_{diss}, r_{ox} and r_{rp} are the rates of gross carbonate dissolution, organic matter remineralization and secondary carbonate reprecipitation, respectively. Fractionation among different dissolved carbonate species is ignored since the majority of the DIC exists in the form of bicarbonate. We also assume that the saturation state of the pore waters with respect to carbonate minerals is at steady-state, hence r_{diss} and r_{rp} do not vary with time.

Because the ultimate driving force for carbonate dissolution is CO_2 input from organic matter oxidation (metabolic dissolution), the net carbonate dissolution rate, $(r_{diss} - r_{rp})$, must equal r_{ox} (e.g., based on the 1:1 stoichiometry shown in rxn. 3). We will also define the re-precipitation ratio R_{rx} as r_{rp}/r_{ox}. Finally we assume that there is no fractionation during organic matter oxidation or carbonate dissolution, and that recrystallization of secondary carbonate occurs under equilibrium conditions with pore water DIC pool. This then implies that

$$R_{rp} = \alpha \times R_{pw} \quad (10)$$

where R_{rp} is the isotopic ratio ($^{13}C/^{12}C$) of the secondary carbonate, subscript pw represents pore water, and α is the fractionation factor between the secondary carbonate phase and bicarbonate ion. Isotopic fractionation ($10^3 \ln\alpha$) between calcite and bicarbonate is 0.9‰ at 25 °C (Rubinson, 1969), and we have therefore used an α value of 1.0009 in these calculations. Finally, F_{rp} equals $R_{rp}/(1 + R_{rp})$.

Eqs. (8) and (9) were solved using a 4th order Runga-Kutta method in the program Stella®. As can be seen in Fig. 10, an increase in the reprecipitation ratio R_{rx} leads to increasingly heavier pore water DIC because of the recycling of primary sediment carbonate (with a $\delta^{13}C$ of 4.0‰) through the DIC pool during dissolution/reprecipitation. If we also combine the approach described in Section 3.2 with these model calculations we can estimate the "apparent" $\delta^{13}C$ of the DIC being added to the pore waters during

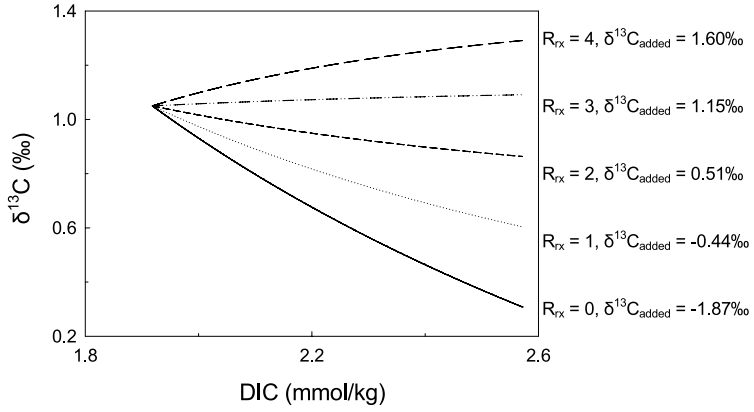

Fig. 10. The closed-system evolution of the $\delta^{13}C$ of pore water DIC with and without carbonate reprecipitation. All of these calculations start with bottom water values, i.e., [DIC] = 1.94 mmol/kg and $\delta^{13}C_{DIC} = 1.1‰$. If no reprecipitation occurs, then the $\delta^{13}C$ of DIC added to the pore waters equals $(\delta^{13}C_{OM} + \delta^{13}C_C)/2 = -1.9‰$. In calculations where reprecipitation occurs, the net dissolution rate was fixed at 0.0163 mmol/kg/h, a value based on our LSI sediment incubations studies (Hu and Burdige, unpubl. data). By varying R_{rx} this then change the gross rate of carbonate dissolution in each calculation.

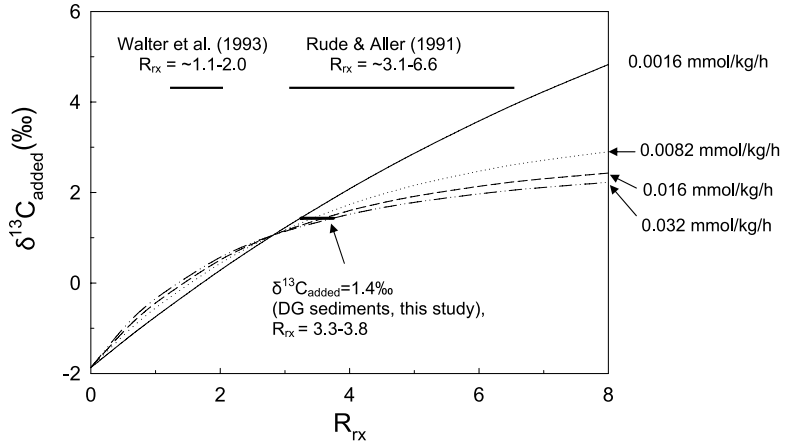

Fig. 11. $\delta^{13}C_{added}$ as a function of R_{rx} and r_{ox}. The two upper horizontal lines represent ranges of R_{rx} from previous studies in Florida Bay sediments (Walter et al., 1993; Rude and Aller, 1991). Values on the right of the plot are r_{ox} values, i.e., net carbonate dissolution rates that range from 10% to 200% of dissolution rates we have observed in LSI sediments (Hu and Burdige, unpubl. data). The lower horizontal line represents the range in R_{rx} for these r_{ox} values based on the $\delta^{13}C_{added}$ value of 1.4‰ observed in the DG sediments.

these simulations. As shown in Fig. 11, this value is a function of not only R_{rx} but also of the absolute rate of net dissolution r_{ox} (particularly for R_{rx} values greater than ~3).

For the dissolution rates in this figure, the value of $\delta^{13}C_{added}$ for the DG sediments "predicts" a value of R_{rx} (3.25–3.75) that is roughly consistent with the range of R_{rx} values for Florida Bay sediments. However, some care must be taken in interpreting this observation since it is not only based on a comparison between closed-system calculations and field observations, but it is also based on a comparison of two very different environments (i.e., "oligotrophic" LSI sediments versus more "eutrophic" Florida Bay sediments). Nevertheless, these model results do suggest that this dissolution/reprecipitation process could explain the $\delta^{13}C$-DIC results from the DG sediments. More detailed open-system modeling of these sediments using a reactive-transport model that consider processes such as pore water advection or diffusion (e.g., Gehlen et al., 1999; McNichol et al., 1991) will be needed to further verify the conclusions reached here regarding carbonate reprecipitation in LSI sediments.

3.3. Why do we see evidence of carbonate reprecipitation only in DG sediments?

The results from the DG sediments appear to provide evidence for the occurrence of carbonate mineral reprecipitation along with dissolution; in contrast no such evidence is seen in the OS and IG sediments. There are at least two explanations for these observations.

The first stems from an examination of the factors that appear to inhibit the inorganic precipitation of calcium carbonate from seawater. The sediment pore waters at these sites, along with much of the surface ocean, are supersaturated with respect to mineral phases such as calcite, and sometime aragonite (Fig. 7 in this study and Morse et al., 1985). However, results from a number of studies suggest that homogeneous precipitation (of calcite at least) is generally inhibited until seawater is even more supersaturated than surface ocean values (e.g., see discussions in Morse et al., 2003). Furthermore, heterogeneous carbonate mineral precipitation from supersaturated solutions may be inhibited because nucleation sites on sediment particles (e.g., carbonate grains) are poisoned by substances such as dissolved organic matter, phosphate, or Mg^{2+} that can adsorb to the nuclei surface (e.g., Berner et al., 1978; Morse and Mackenzie, 1990; Morse and Mucci, 1984; Mucci, 1987). However, in DG sediments with relatively high rates of net carbonate dissolution, the dissolution process may "cleanse" particle surfaces of these inhibitory substances and/or create new nucleation sites. As a result, this may act to overcome the inhibition of carbonate precipitation commonly seen in many laboratory and field studies.

Second, studies of carbonate dissolution and reprecipitation by Hover et al. (2001) suggest that the process may occur through what is termed "Ostwald ripening", in which smaller crystals dissolve and reprecipitate as larger crystals (also see Zullig and Morse, 1988). The driving force for this appears to be the decrease in surface free energy with increasing particle size. Expressed another way, smaller crystals have higher surface free energies and, in a given solution, are therefore more soluble than larger crystals (Walter and Morse, 1985). As a result, during Ostwald ripening, crystals larger than a certain critical radius (representing particles in equilibrium with the solution saturation state) grow at the expense of the dissolution of crystals smaller than this critical radius. The relevance of this to our results may stem from the fact that the overlying seagrass canopy at the DG sites dampens water motion and may enhance the deposition of fine-grained particles relative to that which occurs at the IG and OS sites. The presence of the seagrass canopy may also hinder resuspension and winnowing of fine-grained particles from these sediments. Consistent with these suggestions, Morse et al. (1987) observed that there was up to three times more fine-grained material (<52 μm) in seagrass sediments

relative to unvegetated sands in sites they studied in the Bahamas. The preferential dissolution of this fine-grained material may promote the overall Ostwald ripening of this material in the DG sediments.

Although evidence-to-date suggests that HMC preferentially undergoes net dissolution in LSI sediments (Burdige and Zimmerman, 2002; Hu and Burdige, unpubl. data), the results presented here provide no evidence regarding the composition of the carbonate phase(s) that reprecipitates. Interestingly, the two mechanisms discussed above have the potential to lead to the reprecipitation of difference phases. In the first case (cleansing of nucleation sites), the dissolution of HMC might be expected to result in the reprecipitation of low-Mg calcite (Rude and Aller, 1991). In contrast, Ostwald ripening might be expected to lead to the reprecipitation of HMC with a very similar (although perhaps slightly lower) Mg content relative to the original starting material (Cole and Chakraborty, 2001; Hover et al., 2001). More detailed studies of LSI sediments will be needed to further examine these possibilities.

3.4. Significance of these results

Based on the discussion above, it is likely that carbonate dissolution/reprecipitation may also be responsible for the ^{13}C enrichment seen in the DIC of pore waters from other coastal sediments (Eldridge and Morse, 2000; McNichol et al., 1991). Similarly, carbonate dissolution and reprecipitation may occur in supralysoclinal carbonate-rich deep-sea sediments (Broecker and Clark, 2003; Jahnke and Jahnke, 2004). Thus, it appears that carbonate mineral reprecipitation may be more important than previously thought in the early diagenesis of a wide range of marine sediments.

Returning to shallow water carbonate sediments, these results demonstrate the impact that carbonate dissolution/reprecipitation may have on the isotopic composition of the sediment pore waters. Similar effects are also to be expected for trace elements such as Sr or F, which show differing degrees of incorporation into different carbonate mineral phases (e.g., Rude and Aller, 1991). Furthermore, if reprecipitation is extensive, then the composition of the solids should also evolve with depth (time of burial) from that of the original sediment material (e.g., Patterson and Walter, 1994; Walter et al., 1993). These processes therefore have the potential to significantly impact the paleo-records contained in stable isotope or trace element profiles in carbonate sediments (see discussions in Hover et al., 2001, and references therein). The role of these processes in the overall evolution of carbonate platforms (e.g., Melim et al., 2002) also remains to be further examined.

Acknowledgments

We thank R.C. Zimmerman, R.F. Dias, J. Davis, L. Bodensteiner, S. Kline, and K. Krecek for their assistance with sample collection and analysis, and we also thank Dave Winter in UC Davis for help with carbonate isotope analysis. The staff at Caribbean Marine Research Center provided valuable logistical support and help during our trips to LSI. Drs. Mark Green, Alfonso Mucci and two other anonymous reviewers provided critical comments and suggestions that greatly improved the quality of this manuscript. Financial support was provided by the National Science Foundation Chemical Oceanography Program.

Associate editor: Alfonso Mucci

Appendix A. Derivation of the expression for the $\delta^{13}C$ of the DIC added to sediment pore waters ($\delta^{13}C_{added}$)

We start with a solution of DIC whose concentration is $[DI^{12}C]_0 + [DI^{13}C]_0$ and add α moles of $DI^{12}C$ and β moles of $DI^{13}C$ to this solution. We can then define $\delta^{13}C_{added}$ as,

$$\delta^{13}C_{added} = 10^3\left[\frac{(\beta/\alpha) - R_0}{R_0}\right] \tag{A.1}$$

where R_0 is the $^{13}C/^{12}C$ ratio of the PDB standard. After this carbon addition, [DIC] is given by,

$$\begin{aligned}[DIC] &= [DI^{12}C]_0 + [DI^{13}C]_0 + \frac{\alpha+\beta}{V} \\ &\approx [DI^{12}C]_0 + \frac{\alpha}{V}\end{aligned} \tag{A.2}$$

since $[DI^{12}C]_0 \gg [DI^{13}C]_0$ and $\alpha \gg \beta$ (note that V is the volume of this solution). Similarly, the initial value of $[DIC]\cdot\delta^{13}C$ is given by

$$\begin{aligned}([DIC]\cdot\delta^{13}C)_0 &\approx [DI^{12}C]_0 \cdot 10^3 \\ &\quad\times\left[\frac{[DI^{13}C]_0/[DI^{12}C]_0 - R_0}{R_0}\right] \\ &= 10^3\left[\frac{[DI^{13}C]_0 - R_0[DI^{12}C]_0}{R_0}\right]\end{aligned} \tag{A.3}$$

while its value after this carbon addition is,

$$\begin{aligned}[DIC]\cdot\delta^{13}C &\approx ([DI^{12}C]_0 + \frac{\alpha}{V})\cdot 10^3\left[\frac{\left(\frac{[DI^{13}C]_0+\beta/V}{[DI^{12}C]_0+\alpha/V}\right) - R_0}{R_0}\right] \\ &= 10^3\left[\frac{[DI^{13}C]_0 + (\beta/V) - R_0[DI^{12}C]_0 - R_0(\alpha/V)}{R_0}\right]\end{aligned} \tag{A.4}$$

Taking the differentials of Eqs. (A.2) and (A.4) yields

$$d[DIC] = \frac{\alpha}{V} \tag{A.5}$$

$$d([DIC]\cdot\delta^{13}C) = 10^3\left[\frac{(\beta/V) - R_0(\alpha/V)}{R_0}\right] \tag{A.6}$$

This then implies that if we plot $[DIC]\cdot\delta^{13}C$ versus [DIC], the slope of the best fit line through the data $\left(\frac{d([DIC]\cdot\delta^{13}C)}{d[DIC]}\right)$ will be given by

$$\frac{d([DIC]\cdot\delta^{13}C)}{d[DIC]} = \frac{10^3\left[\frac{(\beta/V)-R_0(\alpha/V)}{R_0}\right]}{\alpha/V} = 10^3\left[\frac{(\beta/\alpha)-R_0}{R_0}\right] \quad (A.7)$$

which based on Eq. (A.1) equals $\delta^{13}C_{added}$.

References

Anderson, W.T., Fourqurean, J.W., 2003. Intra and interannual variability in seagrass carbon and nitrogen stable isotopes from south Florida, a preliminary study. *Org. Geochem.* **34**, 185–194.

Andrews, J.E., 1991. Geochemical indicators of depositional and early diagenetic facies in Holocene carbonate muds, and their preservation potential during stabilisation. *Chem. Geol.* **93**, 267–289.

Berg, P., McGlathery, K.J., 2001. A high-resolution porewater sampling for sandy sediments. *Limnol. Oceanogr.* **46**, 203–210.

Berner, R.A., 1977. Stoichiometric models for nutrient regeneration in anoxic sediment. *Limnol. Oceanogr.* **22**, 781–786.

Berner, R.A., 1980. *Early diagenesis—A Theoretical Approach*. Princeton University Press, Princeton, NJ.

Berner, R.A., Westrich, J.T., Graber, R., Smith, J., Martens, C.S., 1978. Inhibition of aragonite precipitation from supersaturated seawater: a laboratory and field study. *Am. J. Sci.* **278**, 816–837.

Boudreau, B.P., Canfield, D.E., 1993. A comparison of closed- and open-system models for porewater pH and calcite-saturation state. *Geochim. Cosmochim. Acta* **57**, 317–334.

Broecker, W.S., Clark, E., 2003. Pseudo dissolution of marine calcite. *Earth Planet. Sci. Lett.* **208**, 291–296.

Burdige, D.J., 2006. *Geochemistry of Marine Sediments*. Princeton University Press, Princeton, NJ.

Burdige, D.J., Zimmerman, R.C., 2002. Impact of seagrass density on carbonate dissolution in Bahamian Sediments. *Limnol. Oceanogr.* **47**, 1751–1763.

Cai, W.-J., Zhao, P., Wang, Y., 2000. pH and pCO_2 microelectrode measurements and the diffusive behavior of carbon dioxide species in coastal marine sediments. *Mar. Chem.* **70**, 133–148.

Campbell, G., Norman, J., 1998. *An Introduction to Environmental Biophysics*. Springer.

Cline, J.D., 1969. Spectrophotometric determination of hydrogen sulfide in natural waters. *Limnol. Oceanogr.* **14**, 454–458.

Cole, D.R., Chakraborty, S., 2001. 2. Rates and mechanisms of isotopic exchange. In: Valley, J.W., Cole, D.R. (Eds.), *Stable Isotope Geochemistry*. Mineralogical Society of America, Washington, DC.

Craig, H., 1953. The geochemistry of the stable carbon isotopes. *Geochim. Cosmochim. Acta* **3**, 53–92.

Dickson, A.G., Afghan, J.D., Anderson, G.C., 2003. Reference materials for oceanic CO_2 analysis: a method for the certification of total alkalinity. *Mar. Chem.* **80**, 185–197.

Dill, R.F., 1991. Subtidal stromatolites, ooids and crusted-lime mud beds at the Great Bahama Bank Margin, *From Shoreline to Abyss*. SEPM Spec. Pub. No. 46.

DOE, 1994. In: Dickson, A.M. and Goyet, C. (Eds.), *Handbook of Methods For Analysis of the Various Parameters of the Carbonate Dioxide System in Seawater*. Oak Ridge National Laboratory, Oak Ridge, TN, USA.

Eadie, B.J., Jeffrey, L.M., 1973. $\delta^{13}C$ analyses of oceanic particulate organic matter. *Mar. Chem.* **1**, 199–209.

Eldridge, P.M., Morse, J.W., 2000. A diagenetical model for sediments-seagrass interactions. *Mar. Chem.* **70**, 89–103.

Emerson, S., Bender, M., 1981. Carbon fluxes at the sediment–water interface of the deep-sea: calcium carbonate preservation. *J. Mar. Res.* **39**, 139–162.

Gehlen, M., Mucci, A., Boudreau, B., 1999. Modelling the distribution of stable carbon isotopes in porewaters of deep-sea sediments. *Geochim. Cosmochim. Acta* **63**, 2763–2773.

Goldsmith, J.R., Graf, D.L., Heard, H.C., 1961. Lattice constants of the calcium-magnesium carbonates. *Am. Min.* **46**, 453–457.

Gonifiantini, R., Zuppi, G.M., 2003. Carbon isotope exchange rate of DIC in karst groundwater. *Chem. Geol.* **197**, 319–336.

Grasshoff, K., Kremling, K., Ehrhardt, M., 1999. *Methods of Seawater Analysis*. Wiley-VCH.

Green, M.A., Aller, R.C., 1998. Seasonal patterns of carbonate diagenesis in nearshore terrigenous muds: relation to spring phytoplankton bloom and temperature. *J. Mar. Res.* **56**, 1097–1123.

Green, M.A., Aller, R.C., 2001. Early diagenesis of calcium carbonate in Long Island Sound sediments: Benthic fluxes of Ca^{2+} and minor elements during seasonal periods of net dissolution. *J. Mar. Res.* **59**, 769–794.

Hammond, D.E., Giordani, P., Berelson, W.M., Poletti, R., 1999. Diagenesis of carbon and nutrients and benthic exchange in sediments of the Northern Adriatic Sea. *Mar. Chem.* **66**, 53–79.

Hemminga, M.A., Duarte, C.M., 2000. *Seagrass Ecology*. Cambridge University Press, Cambridge.

Hemminga, M.A., Mateo, A.A., 1996. Stable carbon isotopes in seagrasses: variability in ratios and use in ecological studies. *Mar. Ecol. Prog. Ser.* **140**, 285–298.

Holmer, M., Andersen, F.Φ., Nielsen, S.L., Boschker, H.T.S., 2001. The importance of mineralization based on sulfate reduction for nutrient regeneration in tropical seagrass sediments. *Aquat. Bot.* **71**, 1–17.

Hover, V.C., Walter, L.M., Peacor, D.R., 2001. Early marine diagenesis of biogenic aragonite and Mg-calcite: new constrains from high-resolution STEM and AEM analysis of modern platform carbonate. *Chem. Geol.* **175**, 221–248.

Huettel, M., Webster, I.T., 2001. Porewater flow in permeable sediments. In: Boudreau, B.P., Jorgensen, B.B. (Eds.), *The Benthic Boundary Layer: Transport Processes and Biogeochemistry*. Oxford University Press, Oxford.

Jahnke, R.A., Jahnke, D.B., 2004. Calcium carbonate dissolution in deep sea sediments: Reconciling microelectrode, pore water and benthic flux chamber results. *Geochim. Cosmochim. Acta* **68**, 47–59.

Koch, E.W., Gust, G., 1999. Water flow in tide- and wave-dominated beds of the seagrass *Thalassia testudinum*. *Mar. Ecol. Prog. Ser.* **184**, 63–72.

Ku, T.C.W., Walter, L.M., Coleman, M.L., Blake, R.E., Martini, A.M., 1999. Coupling between sulfur recycling and syndepositional carbonate dissolution: evidence from oxygen and sulfur isotope composition of pore water sulfate, South Florida Platform, USA. *Geochim. Cosmochim. Acta* **63**, 2529–2546.

Lewis, E. and Wallace, D., 1998. *Program Developed for CO_2 System Calculations*. ORNL/CDIAC-105. Carbon Dioxide Information Analysis Center, Oak Ridge National Laboratory, U.S. Department of Energy, Oak Ridge, Tennessee., Oak Ridge, Tennessee.

Martin, W.R., McNichol, A.P., McCorkle, D.C., 2000. The radiocarbon age of calcite dissolving at the sea floor: Estimates from pore water data. *Geochim. Cosmochim. Acta* **64**, 1391–1404.

Martin, W.R., Sayles, F.L., 2003. The recycling of biogenic material at the seafloor. In: Machenzie, F.T. (Ed.), *Treatise on Geochemistry*, vol. 7. Elsevier, Amsterdam.

McCorkle, D.C., Emerson, S.R., Quay, P.D., 1985. Stable carbon isotopes in marine porewaters. *Earth Planet. Sci. Lett.* **74**, 13–26.

McMillan, C., 1980. $^{13}C/^{12}C$ ratios in seagrasses. *Aquat. Bot.* **9**, 237–249.

McNichol, A.P., Druffel, E.R.M., Lee, C., 1991. Carbon cycling in coastal sediments: 2. An Investigation of the sources of ΣCO_2 to pore water using carbon isotopes. In: Baker, R.A. (Ed.), *Organic Substances and Sediments in Water*. Lewis Publishers, Chelsea, MI.

Melim, L.A., Westphal, H., Swart, P.K., Eberli, G.P., Munnecke, A., 2002. Questioning carbonate diagenetic paradigms: evidence from the Neogene of the Bahamas. *Mar. Geol.* **185**, 27–53.

Milliman, J.D., Bornhold, B.D., 1973. Peak height versus peak intensity analysis of X-ray diffraction data. *Sedimentology* **20**, 445–448.

Milliman, J.D., Freile, D., Steinen, R.P., Wilber, R.J., 1993. Great Bahama Bank aragonite muds: mostly inorganically precipitated, mostly exported. *J. Sed. Petrol.* **63**, 589–595.

Mook, W.G., de Vries, J.J., 2001. *Environmental Isotopes in the Hydrological Cycle Principles and Applications*, vol. 1. *Introduction: Theory, Methods, Review*. UNESCO/IAEA, Paris.

Morse, J.W., Gledhill, D.K., Millero, F.J., 2003. $CaCO_3$ precipitation kinetics in waters from the Great Bahama Bank: Implications for the relationship between Bank hydrochemistry and whitings. *Geochim. Cosmochim. Acta* **67**, 2819–2826.

Morse, J.W., Mackenzie, F.T., 1990. *Geochemistry of Sedimentary Carbonates*. Elsevier, Amsterdam.

Morse, J.W., Mucci, A., 1984. Composition of carbonate overgrowths produced on Iceland spar calcite crystals buried in Bahamian carbonate-rich sediments. *Sediment. Geol.* **40**, 287–291.

Morse, J.W., Zullig, J.J., Bernstern, L.D., Millero, F.J., Milne, P., Mucci, A., Choppin, G.R., 1985. Chemistry of calcium carbonate-rich shallow water sediments in the Bahamas. *Am. J. Sci.* **285**, 147–185.

Morse, J.W., Zullig, J.J., Iverson, R.L., Choppin, G.R., Mucci, A., Millero, F.J., 1987. The influence of seagrass beds on carbonate sediments in the Bahamas. *Mar. Chem.* **22**, 71–83.

Mucci, A., 1983. The solubility of calcite and aragonite in seawater at various salinities. *Am. J. Sci.* **283**, 780–799.

Mucci, A., 1987. Influence of temperature on the composition of magnesian calcite overgrowths precipitated from seawater. *Geochim. Cosmochim. Acta* **51**, 1977–1984.

Patterson, W.P., Walter, L.M., 1994. Syndepositional diagenesis of modern platform carbonates: evidence from isotopic and minor element data. *Geology* **22**, 127–130.

Plummer, L.N., Sprinkle, C.L., 2001. Radiocarbon dating of dissolved inorganic carbon in groundwater from confined parts of the Upper Floridan aquifer, Florida, USA. *Hydrogeol. J.* **9**, 127–150.

Presley, B.J., Kaplan, I.R., 1968. Changes in dissolved sulfate, calcium and carbonate from interstitial water of near-shore sediments. *Geochim. Cosmochim. Acta* **32**, 1037–1048.

Rasmussen, K.A., Haddad, R.I., Neumann, A.C., 1990. Stable-isotope record of organic carbon from an evolving carbonate banktop, Bight of Abaco, Bahamas. *Geology* **18**, 790–794.

Rubinson, M., 1969. Carbon-13 fractionation between aragonite and calcite. *Geochim. Cosmochim. Acta* **33**, 997–1002.

Rude, P.D., Aller, R.C., 1991. Fluorine mobility during early diagenesis of carbonate sediment: an indicator of mineral transformation. *Geochim. Cosmochim. Acta* **55**, 2491–2509.

Salata, G.G., Roelke, L.A., Cifuentes, L.A., 2000. A rapid and precise method for measuring stable carbon isotope ratios of dissolved inorganic carbon. *Mar. Chem.* **69**, 153–161.

Sampou, P., Oviatt, C.A., 1991. Seasonal patterns of sedimentary carbon and anaerobic respiration along a simulated eutrophication gradient. *Mar. Ecol. Prog. Ser.* **72**, 271–282.

Sayles, F.L., Curry, W.B., 1988. $\delta^{13}C$, TCO_2, and the metabolism of organic carbon in deep sea sediments. *Geochim. Cosmochim. Acta* **52**, 2963–2978.

Scalan, R.S., Morgan, T.D., 1970. Isotope ratio mass spectrometer interumentation and application to organic matter contained in recent sediments. *Int. J. Mass. Spectrom. Ion. Phys.* **4**, 267–281.

Stephens, F.C., Louchard, E.M., Reid, R.P., Maffione, R.A., 2003. Effdects of microalgal communities on reflectance spectra of carbonate sediments in subtidal optically shallow marine environments. *Limnol. Oceanogr.* **48**, 536–546.

Stoessell, R.K., 1992. Effects of sulfate reduction on $CaCO_3$ dissolution and precipitation in mixing-zone fluids. *J. Sed. Petrol.* **62**, 873–880.

Walter, L.M., Bischof, S.A., Patterson, W.P., Lyons, T.W., 1993. Dissolution and recrystallization in modern shelf carbonates: evidence from pore water and solid phase chemistry. *Phil. Trans. R. Soc. Lon.* **344**, 27–36.

Walter, L.M., Burton, E.A., 1990. Dissolution of recent platform carbonate sediments in marine pore fluids. *Am. J. Sci.* **290**, 601–643.

Walter, L.M., Ku, T.C.W., Muehlenbachs, K., Patterson, W.P., and Nonnell, L., 2006. Controls on the $\delta^{13}C$ of dissolved inorganic carbon in marine pore waters: an instructive example from biogenic carbonate sediments (South Florida Platform), *Deep-Sea Res. II*, in press.

Walter, L.M., Morse, J.W., 1984. Magnesian calcite stabilities: a reevaluation. *Geochim. Cosmochim. Acta* **48**, 1059–1069.

Walter, L.M., Morse, J.W., 1985. The dissolution kinetics of shallow marine carbonates in seawater: A laboratory study. *Geochim. Cosmochim. Acta* **49**, 1503–1513.

Zeebe, R.E., Wolf-Gladrow, D., 2001. *CO_2 in Seawater: Equilibrium, Kinetics, Isotopes*. Elsevier, Amsterdam.

Zullig, J.J., Morse, J.W., 1988. Interaction of organic acids with carbonate mineral surfaces in seawater and related solutions: I Fatty acid adsorption. *Geochim. Cosmochim. Acta* **52**, 1667–1678.